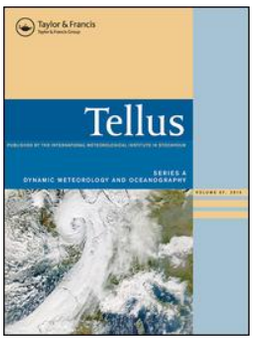

Tellus A: Dynamic Meteorology and Oceanography

ISSN: (Print) 1600-0870 (Online) Journal homepage: http://www.tandfonline.com/loi/zela20

The rôle of orographically and thermally forced stationary waves in the causation of the residual circulation

E. Becker & G. Schmitz

To cite this article: E. Becker & G. Schmitz (1999) The rôle of orographically and thermally forced stationary waves in the causation of the residual circulation, Tellus A: Dynamic Meteorology and Oceanography, 51:5, 902-913, DOI: 10.3402/tellusa.v51i5.14500

To link to this article: https://doi.org/10.3402/tellusa.v51i5.14500

Published online: 27 Jan 2017.

Tellus (1999), 51A, 902–913
Printed in UK – all rights reserved

TELLUS
ISSN 0280–6495

The rôle of orographically and thermally forced stationary waves in the causation of the residual circulation

By E. BECKER* and G. SCHMITZ, *Leibniz-Institute of Atmospheric Physics, Schloßstraße 6, 18225 Kühlungsborn, Germany*

(Manuscript received 31 August 1998; in final form 18 January 1999)

ABSTRACT

Several experiments performed with an idealized troposphere–stratosphere GCM are compared to estimate the impact of orography and prescribed local heat sources on the residual circulation in the northern winter stratosphere. It is found that only the combined action of orographic and thermal wave forcing in northern midlatitudes is capable of inducing a residual circulation reaching continuously from tropical to polar latitudes at stratospheric altitudes. Intensifications of the residual circulation in response to modified forcing of stationary waves are generally associated with, firstly, a reduced polar night jet accompanied by enhanced easterlies in low and summer hemispheric latitudes and, secondly, substantial warming of the polar night stratosphere completely compensated by cooling in the tropics and subtropics.

1. Introduction

The tropical Hadley circulation is one of the classical problems in dynamic meteorology. Nevertheless, understanding its role in global climate remains a challenging problem (Hou, 1993; Hou, 1998; Yang and Webster, 1990; Webster and Chang, 1997). Quantitative models of the Hadley cell trace back to Schneider (1977) and Held and Hou (1980). Owing to the constraint of angular momentum conservation in the poleward branch of the Hadley cell, these authors proposed the intuitive model of a stationary, strictly axisymmetric tropical Hadley circulation separated from middle latitudes; the only physical input was surface friction and temperature relaxation. Held and Hou (1980) proved that the so constructed solution is indeed obtained in a two-dimensional (2D) dynamical model. Several follow-up studies have achieved deeper insight into 2D dynamics, uncovering the sensitivity of the Hadley cell to location and concentration of deep tropical heating (Lindzen and Hou, 1988; Hou and Lindzen, 1992). Dunkerton (1989) investigated the 2D approach for the stratosphere where winter conditions are characterized by a summer to winter pole gradient of the thermal equilibrium temperature.

Realistic three-dimensional (3D) models confirm that the stratospheric residual circulation is primarly driven by planetary waves even though gravity wave drag cannot entirely be neglected (Rosenlof and Holton, 1993). Principally, the annual cycle of the stratospheric temperature reflects the strong orographic and thermal forcing of planetary waves in the northern hemisphere, since these waves propagate into the stratosphere and drive the residual circulation. Comparing the observed climatological residual circulations of January and July yields that, in the northern winter stratosphere, the meridional flow is stronger and also reaches farther into high latitudes (Rosenlof, 1995). Moreover, on the basis of observational data, Yulaeva et al. (1994) have found that the month-to-month changes as well as the annual cylce of the lower-stratospheric

* Corresponding author.

temperature are characterized by a nearly constant horizontal mean temperature. This means, there is an approximate compensation between stratospheric warming in the extratropics and cooling in the tropics and vice versa. For example, in comparison to southern winter, the 10–20 K warmer polar night stratosphere during northern winter is compensated by lower temperatures in the tropical lower stratosphere. Yulaeva et al. (1994) have interpreted such a behavior in terms of a corresponding variability of the residual circulation which, in general, cools the tropics and warms the extratropics. Associated asymmetries between northern and southern winter can be found in the vertical mass fluxes (Holton, 1990) or, most obviously, in the climatological zonal mean zonal winds.

The goal of the present investigation is to study in detail how the stratospheric circulation is affected by the different forcing mechanisms of stationary waves. Our basis is an idealized but nevertheless fairly realistic model of the general circulation in the troposphere and stratosphere (SGCM), including a sponge layer in the lower mesosphere due to enhanced lateral diffusion and additional vertical diffusion of wind. The model design allows a straight forward separation of orographic wave forcing, thermal wave forcing in middle latitudes and thermal wave forcing in the deep tropics. The idealizations ensure that the model response to a perturbation in the wave forcing is not affected by intrinsic interactions between the external forcing fields. Model anomalies are investigated with specific focus on the residual circulation and associated eddy decelerations in the stratosphere. Note that wave propagation into the stratosphere cannot be separated from adjustments in the troposphere, e.g. modifications of zonal wind, temperature and eddy feedback onto the Hadley cell. The tropospheric model response to orographic and thermal wave forcing is analyzed in an associated paper.

The outline of this study is as follows. In Section 2, we briefly describe the model and how experiments have been designed. Additional model details can be found in Becker et al. (1997). Section 3 presents our results with regard to the residual circulation, Eliassen–Palm flux divergence, zonal wind and temperature. In addition we investigate 2D experiments in Subsection 3.4. Finally, Section 4 gives our conclusions.

2. Model design and definition of experiments

The SGCM has a moderate spatial resolution, i.e. spectral truncation at total wave number 29 and 24 hybrid levels extending up to 0.3 mb. Following Hou (1993), we account for radiation and moisture processes in a rather simple way, namely by temperature relaxation and additional prescribed constant heat sources in an otherwise dry atmosphere. Thus, the physics of the model is comprised in the definition of diabatic heating Q and surface temperature T_s:

$$Q := -\frac{T - T_e}{\tau} + Q_c + Q_m + \text{diffusion} \tag{1}$$

$$T_s := \{T_e + \tau(Q_c + Q_m)\}_{\text{lower boundary}}. \tag{2}$$

In (1), τ is relaxation time (16 days in troposphere and stratosphere, 4 days in the uppermost model layers), T temperature and T_e a zonally symmetric equilibrium temperature (Fig. 1). The tropospheric part of our standard T_e (Fig. 1a) corresponds to a typical northern winter state with increased meridional gradients. In the stratosphere, up to about 10 mb, meridional gradients in the winter hemisphere are somewhat weaker than those of the radiatively determined state proposed by Shine (1987). Above 2 mb, the meridional gradient approaches zero to close the model at its top. As a result, the summer hemispheric thermal driving, which in the real atmosphere is maximal at about 1 mb, is not accounted for with the present model version. We are presently testing a version of the SGCM with the vertical resolution extending up to 95 km. In this case, a T_e fairly similar to that proposed by Shine (1987) can be applied. Since in the troposphere and lower stratosphere both model versions generate similar results, we stay with a moderate vertical resolution in this study. It is however open to question whether the present SGCM simulations yield realistic results in the upper stratosphere. Nevertheless, we will present model climatologies up to 1.5 mb.

The prescribed forcing functions Q_c and Q_m mimic convective heating in the deep tropics and latent heating in midlatitudes. Their zonal means (Fig. 2b) are identical in all model experiments. This holds for reasons of consistency also for orography Φ_s (Fig. 2a). Orographic, midlatitude or equatorial thermal forcing of stationary waves

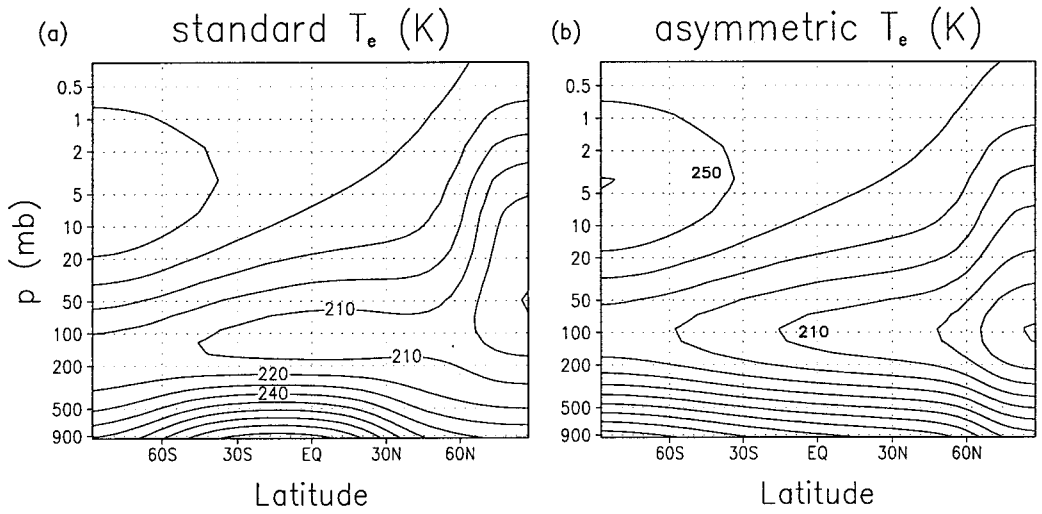

Fig. 1. (a) Standard equilibrium temperature used in all 3D simulations and the equivalent 2D experiment 2D–equi. (b) Equilibrium temperature used in the asymmetric 2D experiments 2D–asym1 and 2D–asym2. The contour internal in each panel is 10 K.

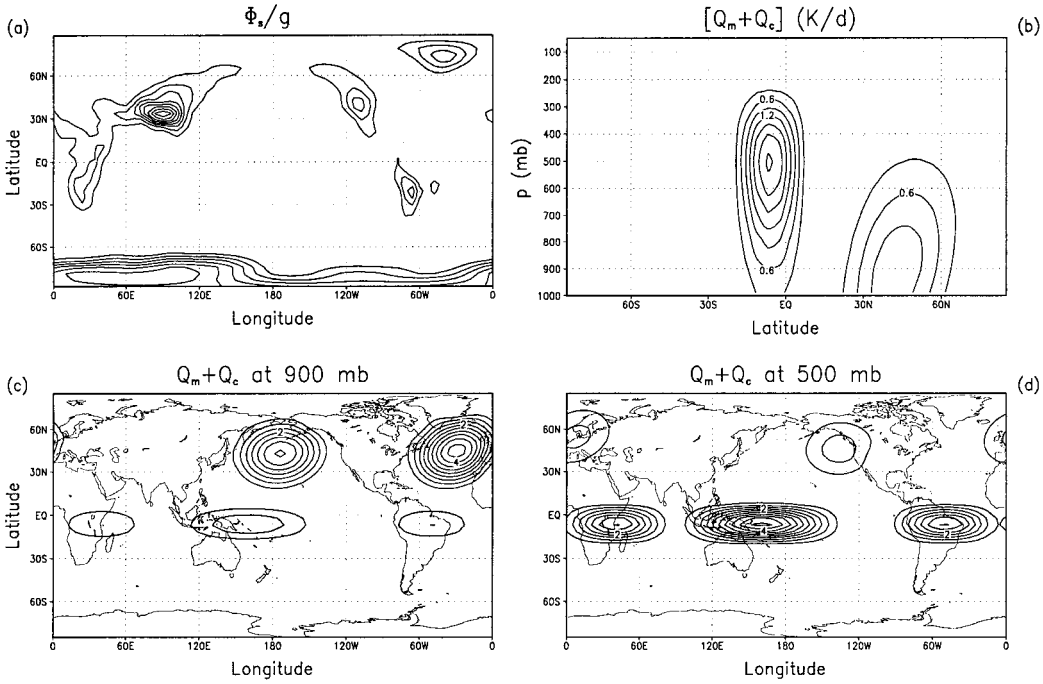

Fig. 2. (a) Orography Φ_s/g. Contours are from 0.5 to 4 km in intervals of 0.5 km. Himalaya and Rockies reach maximum heights of 4.4 and 1.8 km. (b) Zonal mean of additional heating rates Q_m and Q_c (contour interval 0.3 K/d). (c),(d) Longitude-dependencies of additional heating rates Q_m and Q_c at 900 and 500 mb. Contours are from 0.5 to 5 K/d in intervals of 0.5 K/d.

is realized by substituting a zonally symmetric external field $[\Phi_s]$, $[Q_m]$ or $[Q_c]$ by its longitude-dependent counterpart $\Phi_s(\lambda)$, $Q_m(\lambda)$ or $Q_c(\lambda)$. The longitude-dependencies of Q_m and Q_c are illustrated in Figs. 2c, d. Q_m is located in the geographical regions of the warm ocean currents and shifts downstream with increasing altitude. The maxima of Q_c represent the three major tropical convection zones for northern winter conditions.

Turbulent boundary layer mixing is parameterized by the local vertical diffusion scheme described in Holtsag and Boville (1993) and also used in Becker et al. (1997). The dynamic boundary condition is formulated with a constant roughness length of 10^{-3} m. Land–sea differences are accounted for in the vertical diffusion scheme via defining the surface temperature (2) as the effective equilibrium temperature

$$T_{e\text{-}eff} := T_e + \tau(Q_c + Q_m) \tag{3}$$

evaluated at the lower boundary. The model includes an ordinary ∇^4-horizontal diffusion scheme with total wavenumber 29 time constants of 2, 1 and 2 days for vorticity, divergence and temperature. Wave reflection from the upper boundary is suppressed by enhanced horizontal diffusion in the uppermost 4 model layers. The onset of gravity wave drag in the upper stratosphere is included by additional vertical diffusion of wind (Matsuno, 1982), with the prescribed kinematic viscosity profile amounting to 10 m^2/s at 0.3 mb and sloping down to zero below (solid line in Fig. 3).

We will consider 4 different long-time model runs (3240 day integrations preceeded by sufficiently long spin–up times). The respective model configurations are abbreviated by writing the external forcing fields either in brackets or as function of longitude λ. We start with the rotationally invariant reference run $[\Phi_s]/[Q_m]/[Q_c]$ and accomplish the model setup by taking orographic forcing (run $\Phi_s(\lambda)/[Q_m]/[Q_c]$), midlatitude thermal forcing (run $\Phi_s(\lambda)/Q_m(\lambda)/[Q_c]$) and equatorial thermal forcing (run $\Phi_s(\lambda)/Q_m(\lambda)/Q_c(\lambda)$) of stationary waves successively into account. In case of orographic and midlatitude thermal wave forcing, integration intervals of a few 1000 days are required to approximately average out the effects of internal variability in the stratosphere. In the troposphere, the model response is stable for integration intervals of a few hundred days.

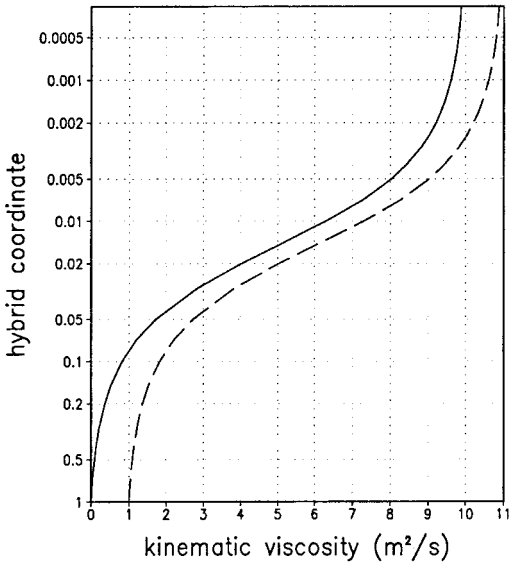

Fig. 3. Prescribed additional kinematic viscosity as a function of the vertical hybrid coordinate. Solid and dashed lines correspond to 3D and 2D experiments.

In addition, we inspect three 2D simulations. For simplicity we have induced further idealizations in the 2D model setup. The boundary layer parameterization is substituted by a linear surface drag like in the numerical 2D model of Held and Hou (1980), vertical diffusion of potential temperature and midlatitude heating Q_m are omitted and the prescribed kinematic viscosity profile corresponds to the dashed line in Fig. 3. In the first 2D run, abbreviated as 2D–equi, the model setup is otherwise equivalent to the 3D reference experiment $[\Phi_s]/[Q_m]/[Q_c]$. In the remaining 2D experiments, denoted as 2D–asym1 and 2D–asym2, our standard equilibrium temperature (Fig. 1a) is exchanged by the asymmetric T_e given in Fig. 1b. This model setup is designed to correspond to the reference experiment of Dunkerton (1989, Fig. 7) where the meridional gradient of T_e is constant throughout the entire atmosphere. In order to explore the role of convective heating in the deep tropics, $[Q_c]$ is neglected in run 2D–asym1 but included in run 2D–asym2.

3. Results

3.1. Residual circulation

Fig. 4 shows the residual mass streamfunction in quasi-geostrophic approximation, calculated

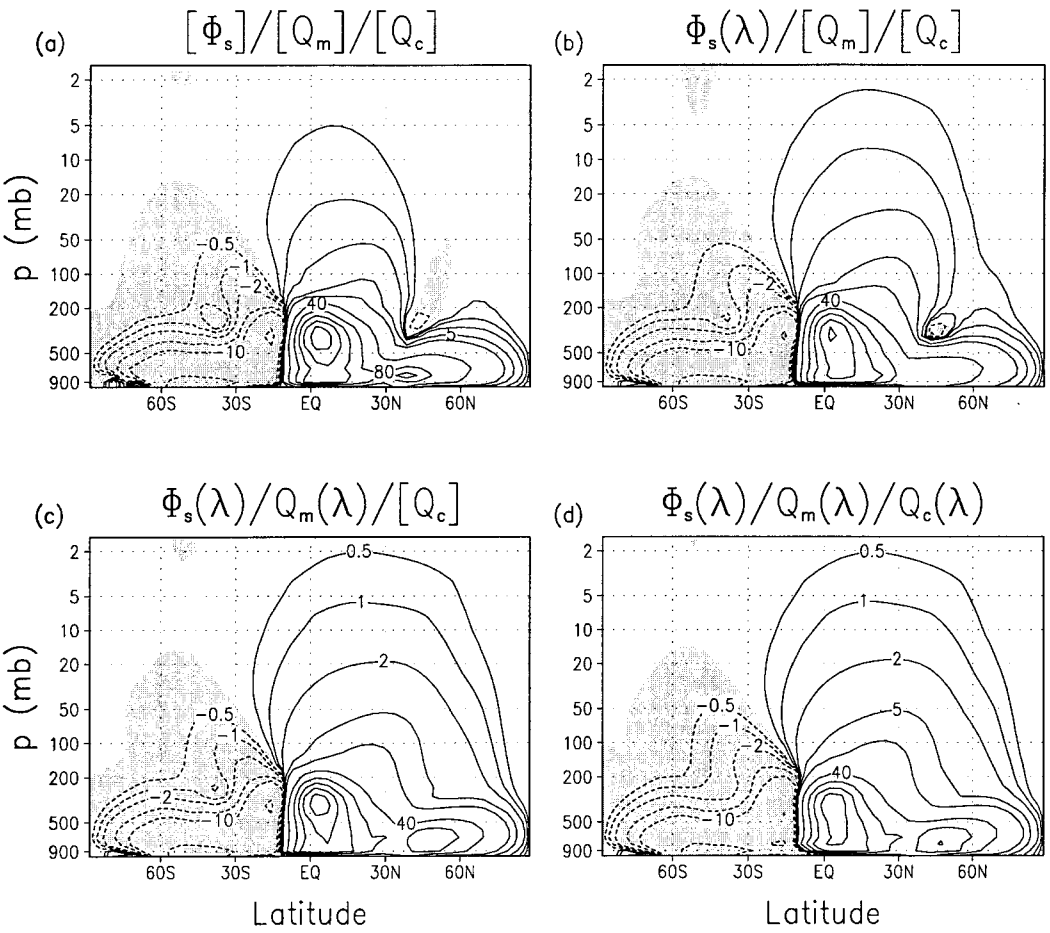

Fig. 4. Residual mass streamfunction for experiments with different forcings of stationary waves. The model configuration is defined in the title of each panel. Contours are ± 0.5, 1, 2, 5, 10, 40, 80, ..., $\times 10^9$ kg/s. Zero contours are not drawn and negative values are shaded.

according to Edmon et al. (1980, eq. (3.4)). Let us consider the stratosphere first.

From Fig. 4a, we see that even without any stationary waves there is a significant residual circulation reaching from the tropics to low midlatitudes. However, in absence of orographically and thermally forced stationary waves, 3D dynamics generates no stratospheric circulation at higher latitudes. The situation is somewhat different when orographic waves come into play (Fig. 4b). Then, both the subtropical branch and the high latitude branch of the residual streamfunction reach farther into the stratosphere. The negative spot in the upper troposphere around 40°N is maintained.

The response to thermally forced midlatitude stationary waves can be deduced by comparing Figs. 4b, c. The most obvious effect is a substantial intensification of the residual mass flux into middle and high latitudes. An additional model experiment with midlatitude thermal wave forcing but zonally symmetric orography (not shown) reveals that only the combination of orographic and midlatitude thermal wave forcing is sufficient to generate a continuously stratospheric mass flux from low to high latitudes. From Fig. 4d it follows that thermal wave forcing in the deep tropics has no significant impact onto the stratospheric residual circulation.

Streamfunction calculations of Rosenlof (1995) have shown that, in the southern winter strato-

sphere, the residual circulation is substantially weaker compared to its northern winter counterpart. And furthermore, streamlines slope down into the troposphere already in the subtropics and middle latitudes, while the northern winter residual circulation reaches polar latitudes at stratospheric altitudes. Figs. 4a, d are consistent with these results, provided the rotationally invariant and the full wave forcing experiment are considered to be representative for the southern and the northern winter stratosphere.

In the troposphere, the residual circulation shows various alterations of the Hadley cell. The effects are visible as well in the Eulerian frame and are discussed in more detail in an associated study. Orographic wave forcing causes a reduction of the streamfunction maximum while the Hadley circulation becomes stronger at low altitudes. With regard to comparison of idealized 2D and 3D simulations (Becker et al., 1997), such an effect indicates enhanced feedback of midlatitude eddies onto the Hadley cell. The consequence of midlatitude thermal forcing is quite opposite. The streamfunction concentrates around the enhanced maximum, indicating reduced eddy feedback. The residual circulation also reaches farther into middle and high latitudes of the troposphere in response to midlatitude thermal wave forcing. The Hadley cell maximum is reduced again when tropical heating is concentrated at certain longitudes as defined in Fig. 2. Such an effect occurs in an idealized model due to increased static stability in those geographical regions where the Hadley circulation is strongest.

3.2. *Eliassen–Palm flux divergence*

Fig. 5 shows the Eliassen–Palm flux divergence for the four 3D experiments using the approximation of Edmon et al. (1980, eq. (3.12)). Comparing the different cases provides evidence that intensifications of the residual circulation in middle and high latitudes as deduced from Fig. 4 are indeed consequences of enhanced eddy activity. The stratospheric Eliassen–Palm flux convergence maximum is intensified and extends farther poleward in response to both orographic and midlatitude thermal forcing of stationary waves. The convergence maximum in the poleward branch of the Hadley cell also undergoes significant changes, confirming that eddy mixing increases due to orographic wave forcing and decreases due to midlatitude thermal wave forcing. Comparison of Figs. 5c, d also yields an anomalous eddy acceleration in the rising branch of the Hadley cell in response to equatorial thermal wave forcing. This effect is associated with the Walker circulation generated in run $\Phi_s(\lambda)/Q_m(\lambda)/Q_c(\lambda)$ and not further addressed here.

3.3. *Zonal wind*

The anomalous eddy decelerations along streamlines of the residual flow (Figs. 4, 5) imply significant changes of the zonal mean zonal wind. This is illustrated in Fig. 6. Comparing Figs. 6a, b yields that orographic wave forcing causes a poleward shift of the whole northern hemispheric wind maximum. The tropospheric jet is clearly reduced by about 10 m/s. The fact that midlatitude thermal wave forcing gives rise to a strongly intensified residual circulation and Eliassen–Palm flux convergence especially at high latitudes is reflected in Fig. 6c by a substantial reduction of the polar night jet by more than 30 m/s. Also the tropospheric jet is reduced by 10 m/s. Consistent with the slight anomalies of the residual circulation and Eliassen–Palm-flux divergence in the winter stratosphere in response to longitude-dependent tropical heating, the changes of the zonal wind are weak when comparing Figs. 6c, d. The main anomaly is present in the upper polar night stratosphere where the model behavior may not be fairly realistic. A westerly anomaly is visible in the deep tropics between 500 and 200 mb. This effect is again connected with the Walker circulation and analysed in detail in an associated paper.

Generally, every angular momentum reduction associated with the polar night jet is accompanied by enhanced easterlies in low latitudes. Thus, the zonal winds of both the rotationally invariant and the full-wave forcing experiment (Figs. 6a, d) reproduce qualitatively the observed stratospheric asymmetry between southern and northern winter.

3.4. *Angular momentum conservation and 2D experiments*

The question to what extent wave processes change the 2D picture of angular momentum conservation can well be illuminated by plotting the residual mass streamfunction together with

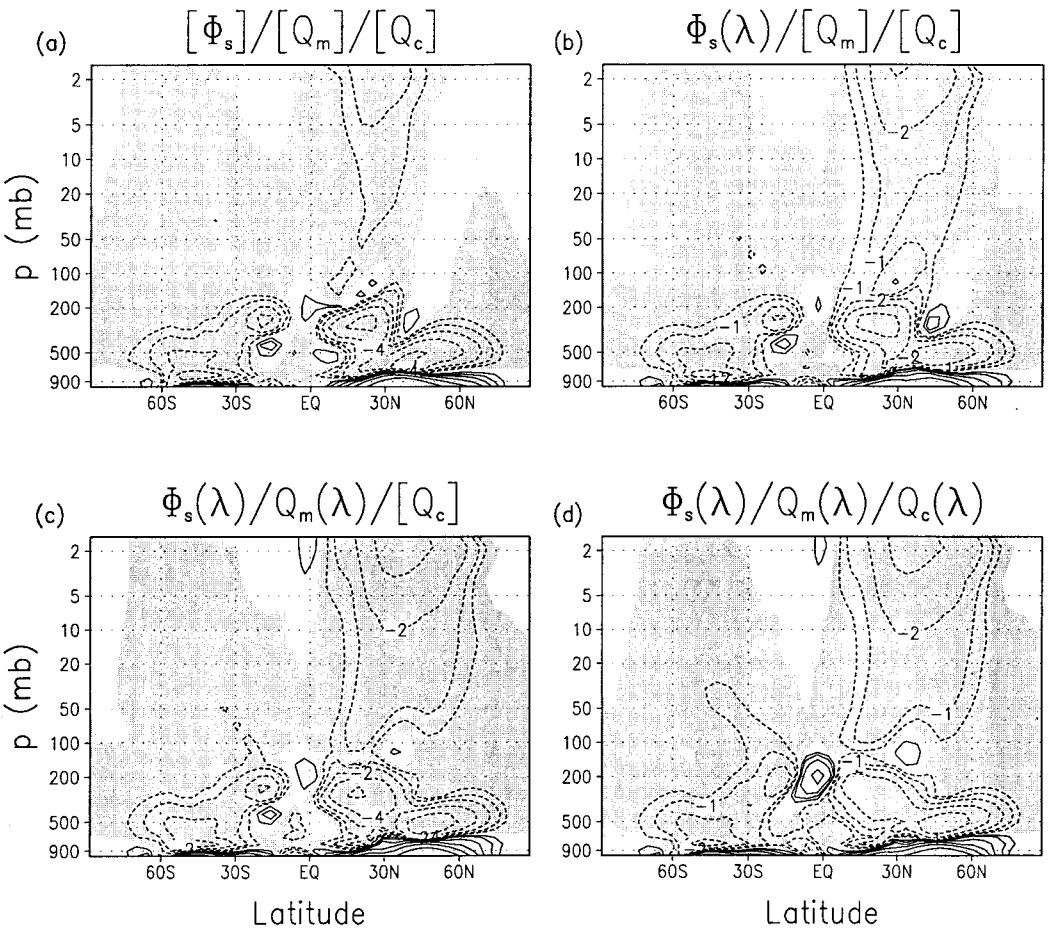

Fig. 5. Same as Fig. 4, but for the Eliassen–Palm-flux divergence. Contours are ± 0.5, 1, 2, 4, 8, 16×10^{15} m^3.

contours of constant zonal angular momentum. This has been done in Fig. 7a for the full wave forcing experiment and in Figs. 7b–c for the 3 2D experiments. Fig. 7a demonstrates that the residual circulation approximately conserves angular momentum only in the rising branch of the Hadley cell. In the extratropical poleward branch, streamlines and momentum contours are almost perpendicular. In 3D dynamics, we generally observe that the extratropical residual flow is far from angular momentum conservation.

Figs. 7a, b are consistent with corresponding 3D and 2D experiments of Becker et al. (1997). In the equivalent 2D experiment, the tropical mass circulation is much stronger than in 3D and concentrates in the middle and upper troposphere. The 2D simulation confirms that the Hadley circulation is to a good approximation angular momentum conserving. In the 3D run (Fig. 7a), the highest contour of angular momentum (450 m/s $\times$ earth radius) intersects the tropical atmosphere twice. In contrast, the 450 contour is pushed out of the Hadley regime in the equivalent 2D run (Fig. 7b). It is important to note that the 2D experiment does not yield a Hadley regime in the stratosphere. The $\pm 0.5 \times 10^9$ kg/s streamfunction contours rather indicate vertically alternating meridional cells in the equatorial stratosphere. These stationary cells become more obvious from the corresponding meridional velocity which is

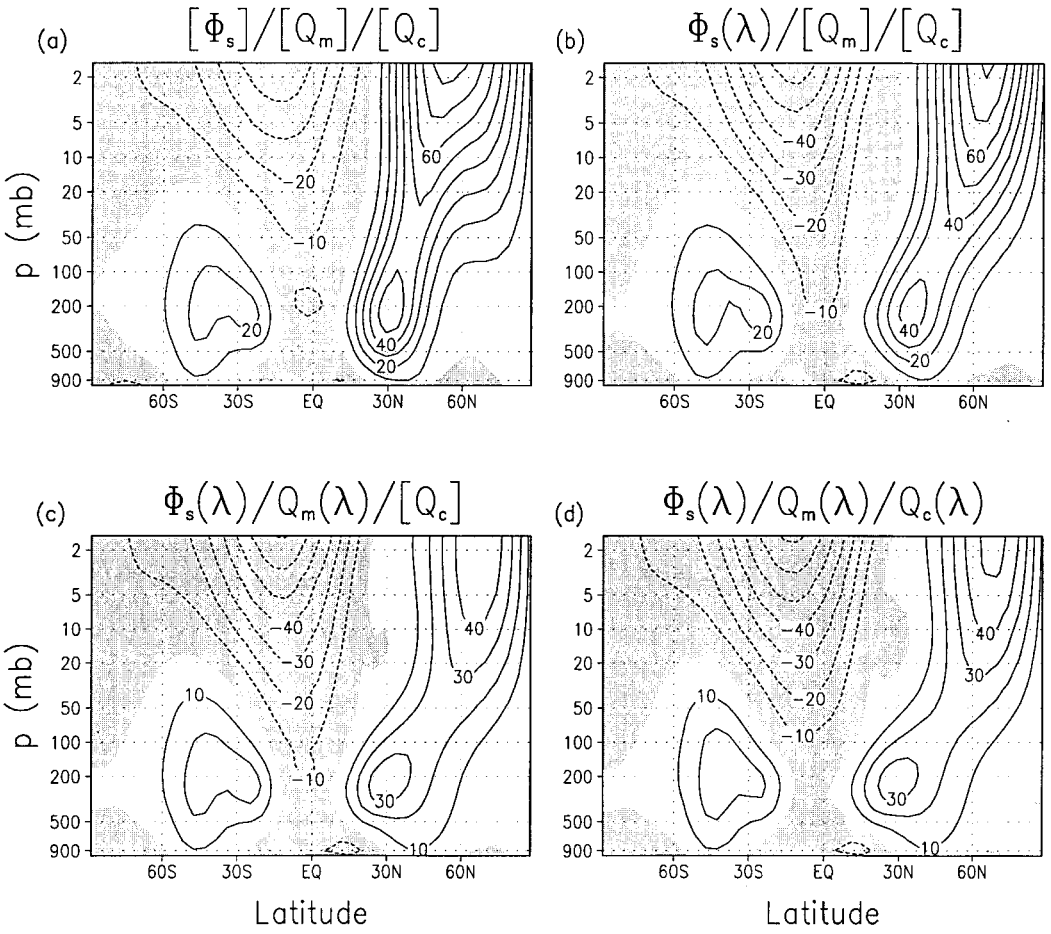

Fig. 6. Same as Fig. 4, but for the zonal mean zonal wind. The contour interval is 10 m/s.

not shown here. They are associated with inertial instability of the zonal flow which, in the present 2D experiment, is not resolved by a reasonable physical process. As pointed out by Dunkerton (1989), some kind of meridional circulation must exist in the stratosphere since a cross-equatorial temperature gradient cannot be thermally balanced by any zonal wind. In our 3D experiments, inertia oscillations are generally absent. In 2D, they can be smoothed out by increasing the prescribed kinematic viscosity. As a result, one obtains a stratospheric meridional circulation where Coriolis force and nonlinear advection are strongly balanced by friction.

Seemingly, there is a discrepancy to a 2D simulation performed by Dunkerton (1989) who noted that "there exists a nonlinear Hadley regime driven by thermal equilibria typical of the middle atmosphere at the solstices". However, our effective equilibrium temperature (3) has fundamentally different meridional gradients in troposphere and stratosphere while Dunkerton (1989) used the same meridional dependence of $T_{\text{e-eff}}$ in both atmospheric layers. Therefore, the equivalent 2D simulation shown in Fig. 7b is not necessarily comparable with Dunkerton's 2D simulation.

In run 2D–asym1, (Fig. 7c) tropical heating is neglected and the asymmetric equilibrium temperature (Fig. 1b) is employed. Note that for this model setup the cross-equatorial gradient $\partial_y T_{\text{e-eff}}$

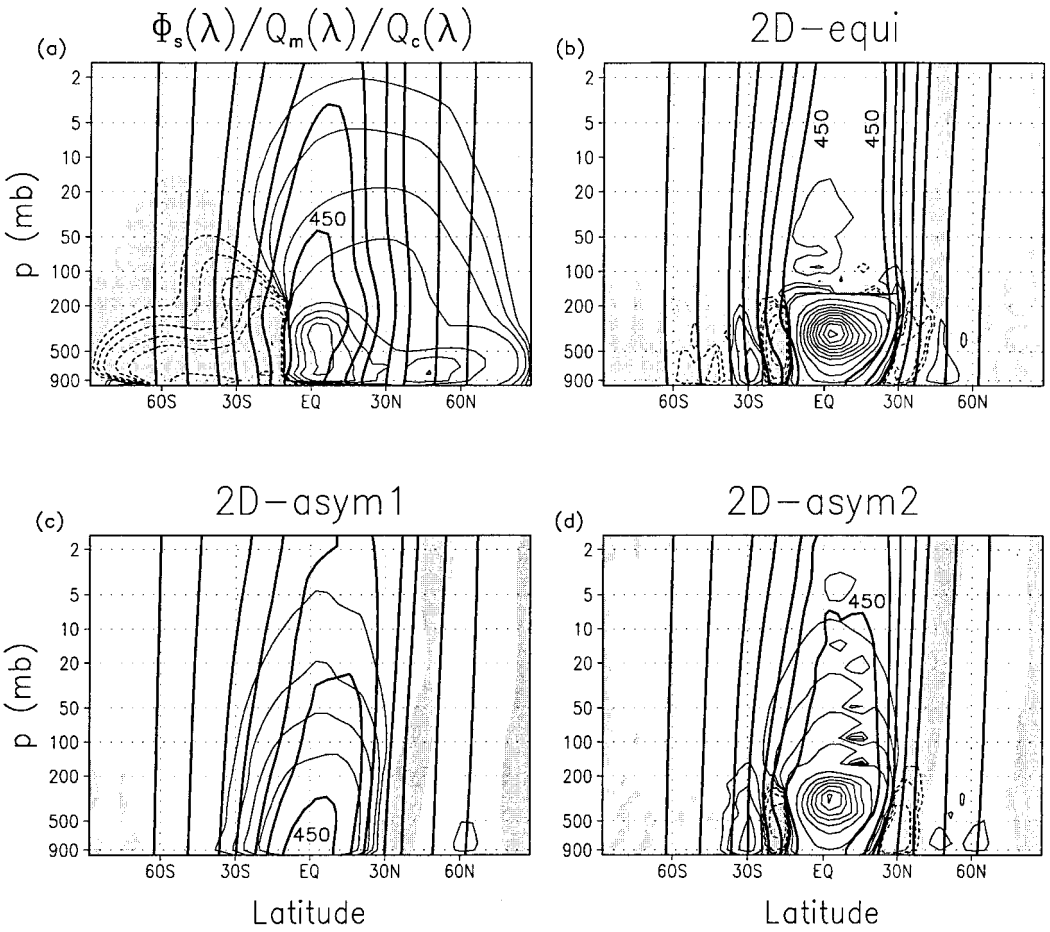

Fig. 7. (a) Residual mass streamfunction superposed with contours of constant angular momentum for the 3D simulation with full longitude-dependent external forcing. (b) Meridional mass streamfunction superposed with contours of constant angular momentum for the equivalent 2D experiment. (c) Same as (b), but for the asymmetric 2D experiment with T_e given in Fig. 1b and tropical heating Q_c neglected. (d) Same as (c), but with tropical heating Q_c included. Contours of the mass stream-functions are as in Fig. 4. Zonal angular momentum divided by the earth radius is indicated by thick contours which are drawn for 100, 200, 300, 350, 400, 425 and 450 m/s. The 450 m/s contour is labeled in each panel.

is almost independent from altitude. The resulting Hadley circulation clearly extends beyond the tropopause even though the streamfunction maximum is considerably weak due to vanishing tropical heating Q_c. Deviations from angular momentum conservation are due to the action of vertical diffusion. One may argue that the occurence of a stratospheric Hadley regime in run 2D–asym1 results from the stronger $\partial_y T_{e\text{-}eff}$ in the region of the tropical tropopause (Fig. 1b) in comparison to that used in run 2D–asym (Fig. 1a). However, if we change the tropospheric thermal equilibrium again by including tropical heating Q_c (run 2D–asym2, Fig. 7d), a vigorous tropospheric Hadley cell is generated analogously to run 2D–equi while vertically alternating meridional winds occur in the equatorial stratosphere. These results may be summarized as follows: If the cross-equatorial gradient $\partial_y T_{e\text{-}eff}$ decreases strongly from troposphere to stratosphere, a nonlinear stratospheric Hadley regime does hardly exist in a 2D dynamical model.

3.5. *Temperature*

Consistent with thermal wind balance, substantial anomalies to changes in the wave forcing configuration can also be found in the zonal mean temperatures. These are shown for the four 3D experiments in Fig. 8 by thin contours. Superposed thick contours in Figs. 8b–d indicate temperature anomalies relative to the rotationally invariant reference run (Fig. 8a). From Fig. 8b we see that orographically forced stationary waves induce a moderate temperature signal. The combined effect of orographic and midlatitude thermal forcing gives rise to a strong warming of the polar night stratosphere exceeding 20 K in the SGCM (Fig. 8c). In the upper stratosphere, the temperature signal is somewhat reduced in response to thermal wave forcing in the deep tropics (Fig. 8d). In each case the high latitude warming is accompanied by cooling in the tropical and subtropical region. The temperature signals in Figs. 8c or d reproduce roughly the observed asymmetry between the southern and the northern winter stratosphere.

As already mentioned in the introduction, observed zonal mean temperature variations in the lower stratosphere show an almost complete compensation between cooling in low and warming in high latitudes. Moreover, the compensation can consistently be interpreted by anomalous

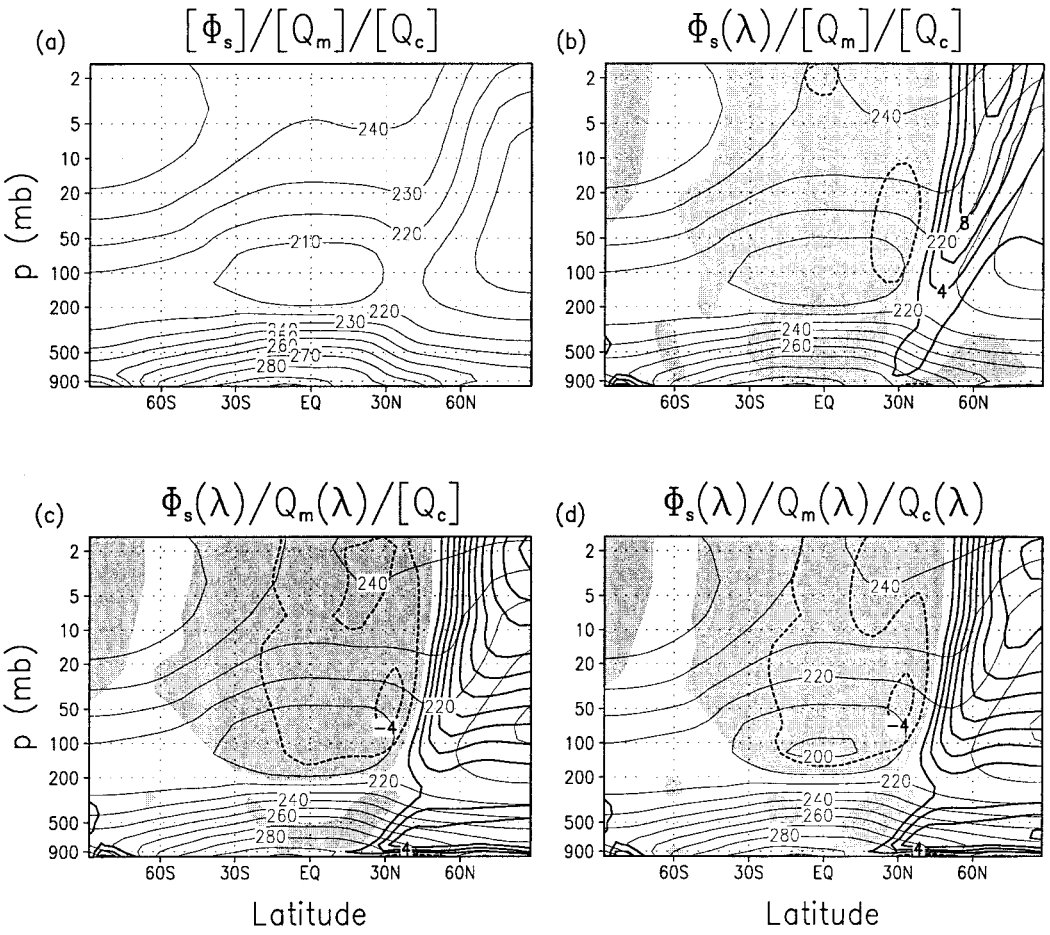

Fig. 8. Zonal mean temperature (thin contours, contour interval 10 K) for experiments with different forcings of stationary waves. The model configuration is defined in the title of each panel. In (b)–(d), the temperature anomaly relative to (a) is indicated by thick contours (interval 2 K) with negative values shaded and zero contours not drawn.

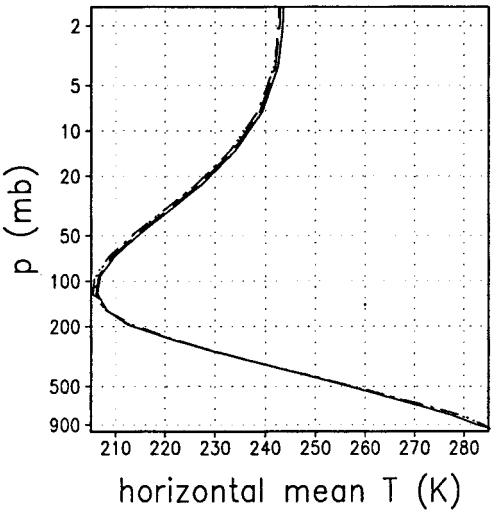

Fig. 9. Horizontal mean temperatures for experiments with different forcings of stationary waves as defined in section 2: $[\Phi_s]/[Q_m]/[Q_c]$ (solid), $[\Phi_s](\lambda)/[Q_m]/[Q_c]$ (dashed), and $[\Phi_s](\lambda)/Q_m(\lambda)/Q_c(\lambda)$ (dashed–dotted)

dynamic cooling and heating rates brought about by corresponding changes of the residual circulation (Yulaeva et al., 1994). The high correspondence between temperature signals and alterations of the residual circulation in our simulations provides further evidence for such a mechanism. Fig. 9 indeed confirms that the vertical profiles of the horizontal mean temperature are almost identical for the four SGCM experiments, especially in the stratosphere.

4. Conclusions

With specific focus on the stratosphere, we have studied the impact of stationary waves onto the zonally averaged circulation. Our basis has been formed by January simulations performed with an idealized troposphere–stratosphere GCM, allowing for a straight forward separation of the three major forcing mechanisms of stationary waves.

Relative to rotationally invariant conditions, orographic forcing of stationary waves gives rise to a stronger residual circulation in the stratosphere. However, separation of orographic and midlatitude thermal wave forcing reveals that only the combined effect of both longitude-dependencies induces a continuously stratospheric mass transport from low to polar latitudes, as it is observed for the northern winter hemisphere. Orographic wave forcing alone does not change the aqua-planet circulation pattern qualitatively, and streamlines of the residual flow slope down into the troposphere already in middle latitudes. Such a behavior is typical for the southern winter stratosphere (Rosenlof, 1995).

In the stratosphere, a stronger residual circulation is associated with a reduced polar night jet accompanied by enhanced easterlies in low latitudes and warming in the winter hemispheric extratropics which is completely compensated by cooling in the tropical and subtropical region (Figs. 4, 6, 8). These connections fit quite well to the observed asymmetries in zonal wind and temperature when comparing southern winter and northern winter climatologies.

In 3D simulations, any residual circulation in the winter stratosphere is far from angular momentum conservation (Fig. 7a). In low viscous 2D dynamics, a nonlinear (i.e. approximately angular momentum conserving) stratospheric Hadley regime is obtained if the meridional gradient of the effective equilibrium temperature is similar in troposphere and stratosphere (Fig. 7c). For realistic thermal forcing, the cross-equatorial gradient of thermal equilibrium decreases strongly from troposphere to stratosphere due to the finite depth of tropical cumulus heating. In this case, a vigorous Hadley circulation exists in the troposphere while standing inertia oscillations occur in the stratosphere (Figs. 7b, d).

Diabatic heating in the tropical troposphere is almost the same in the equivalent 2D run and in all 3D experiments. Hence, the vertical mass fluxes into the tropical lower stratosphere are entirely determined by wave activity in the extratropics. Therefore, the present SGCM experiments provide further evidence for the concept of the extratropical "wave pump" (Holton et al., 1995), confirming that planetary waves which drive the residual circulation in the extratropical stratosphere induce upwelling in the tropics. This mechanism is also reminescent of the tropospheric feedback of midlatitude waves onto the Hadley cell in case of weak tropical heating (Becker et al., 1997, Fig. 2).

Owing to the complete compensation in the temperature anomalies (Figs. 8, 9) and the fact that our 3D simulations differ only with respect

to longitude-dependent components of prescribed external forcing fields, the following conclusion is obvious. The stratospheric temperature signals are caused by modified stationary wave forcing in the lower troposphere; they reflect enhanced heat exchange between the tropical and the extratropical stratosphere brought about by intensifications of the residual circulation as proposed by Yulaeva et al. (1994).

This suggests a crucial dependence of the stratospheric temperature distribution upon moisture processes in lower troposphere. Furthermore, deficiencies of advanced troposphere–stratosphere GCMs in predicting realistic temperatures and winds in the polar night stratosphere may be attributed, at least partly, to uncertainties in the parameterization of convective and latent heating.

5. Acknowledgement

For valuable discussions we would like to thank A. Gabriel and C.-O. Hinrichs. Comments of K. K. Tung and A. Y. Hou are gratefully acknowledged. This work was partially supported by the Bundesministerium für Bildung, Forschung und Technologie under 07VKV01/1,23.

REFERENCES

Becker, E., Schmitz, G. and Geprägs, R. 1997. The feedback of midlatitude waves onto the Hadley cell in a simple general circulation model. *Tellus* **49A**, 182–199.

Dunkerton, T. J. 1989. Nonlinear Hadley circulation driven by asymmetric differential heating. *J. Atmos. Sci.* **46**, 956–974.

Edmon, Jr., H. J., Hoskins, B. J. and McIntyre, M. E. 1980. Eliassen–Palm cross sections for the troposphere. *J. Atmos. Sci.* **37**, 2600–2616.

Held, I. M. and Hou, A. Y. 1980. Nonlinear axially symmetric circulations in a nearly inviscid atmosphere. *J. Atmos. Sci.* **37**, 515–533.

Holton, J. R. 1990. On the global exchange of mass between the stratosphere and troposphere. *J. Atmos. Sci.* **47**, 392–395.

Holton, J. R., Haynes, P. H., McIntyre, M. E., Douglass, A. R., Rood, R. B. and Pfister, L. 1995. Stratosphere–troposphere exchange. *Rev. Geophys.* **33**, 403–439.

Holtslag, A. A. M. and Boville, B. A. 1993. Local versus nonlocal boundary-layer diffusion in a global climate model. *J. Climate* **6**, 1825–1842.

Hou, A. Y. 1993. The influence of tropical heating displacements on the extratropical climate. *J. Atmos. Sci.* **50**, 3553–3570.

Hou, A. Y. 1998. Hadley circulation as a modulator of the extratropical climate. *J. Atmos. Sci.* **55**, 2437–2457.

Hou, A. Y. and Lindzen, R. S. 1992. The influence of concentrated heating on the Hadley circulation. *J. Atmos. Sci.* **49**, 1233–1241.

Lindzen, R. S and Hou, A. Y. 1998. Hadley circulations for zonally averaged heating centered off the equator. *J. Atmos. Sci.* **45**, 2416–2427.

Matsuno, B. 1982. A quasi-one-dimensional model of the middle atmosphere circulation interacting with internal gravity waves. *J. Meteor. Soc. Japan* **60**, 215–226.

Rosenlof, K. H. 1995. Seasonal cycle of the residual mean meridional circulation in the stratosphere. *J. Geophys. Res.* **100**, 5173–5191.

Rosenlof, K. H. and Holton, J. R. 1993. Estimates of the stratospheric residual circulation using the downward control principle. *J. Geophys. Res.* **98**, 10465–10479.

Schneider, E. K. 1977. Axially symmetric steady-state models of the basic state for instability and climate studies. Part II. Nonlinear calculations. *J. Atmos. Sci.* **34**, 280–296.

Shine, K. P. 1987. The middle atmosphere in the absence of dynamical heat fluxes. *Quart. J. R. Met. Soc.* **113**, 603–633.

Webster, P. J. and Chang, H.-R. 1997. Atmospheric wave propagation in heterogeneous flow: basic flow controls on tropical–extratropical interaction and equatorial wave modification. *Dyn. Atmosph. Oceans* **27**, 91–134.

Yang, S. and Webster, P. J. 1990. The effect of summer tropical heating on the location and intensity of the extratropical westerly jet streams. *J. Geophys. Res.* **95** 18705–18721.

Yulaeva, E., Holton, J. R. and Wallace, J. M. 1994. On the cause of the annual cycle in tropical lower-stratospheric temperatures. *J. Atmos. Sci.* **51**, 169–174.